

## Endogenous viral elements reveal associations between a non-retroviral RNA virus and symbiotic dinoflagellate genomes

Alex J. Veglia  <sup>1,23</sup>, Kalia S. I. Bistolas  <sup>2,23</sup>✉, Christian R. Voolstra  <sup>3</sup>, Benjamin C. C. Hume  <sup>3</sup>, Hans-Joachim Ruscheweyh  <sup>4</sup>, Serge Planes <sup>5</sup>, Denis Allemand  <sup>6</sup>, Emilie Boissin  <sup>5</sup>, Patrick Wincker  <sup>7,8</sup>, Julie Poulain <sup>7,8</sup>, Clémentine Moulin <sup>9</sup>, Guillaume Bourdin  <sup>10</sup>, Guillaume Iwankow <sup>5</sup>, Sarah Romac <sup>11</sup>, Sylvain Agostini  <sup>12</sup>, Bernard Banaigs <sup>5</sup>, Emmanuel Boss  <sup>10</sup>, Chris Bowler  <sup>13</sup>, Colomban de Vargas <sup>11</sup>, Eric Douville  <sup>14</sup>, Michel Flores  <sup>15</sup>, Didier Forcioli  <sup>16,17</sup>, Paola Furla  <sup>16,17</sup>, Pierre E. Galand  <sup>18</sup>, Eric Gilson  <sup>16,19</sup>, Fabien Lombard  <sup>20</sup>, Stéphane Pesant <sup>21</sup>, Stéphanie Reynaud  <sup>6</sup>, Shinichi Sunagawa  <sup>4</sup>, Olivier P. Thomas <sup>22</sup>, Romain Troublé  <sup>9</sup>, Didier Zoccola  <sup>6</sup>, Adrienne M. S. Correa  <sup>1</sup> & Rebecca L. Vega Thurber  <sup>2</sup>

Endogenous viral elements (EVEs) offer insight into the evolutionary histories and hosts of contemporary viruses. This study leveraged DNA metagenomics and genomics to detect and infer the host of a non-retroviral dinoflagellate-infecting +ssRNA virus (dinoNAV) common in coral reefs. As part of the Tara Pacific Expedition, this study surveyed 269 newly sequenced cnidarians and their resident symbiotic dinoflagellates (Symbiodiniaceae), associated metabarcodes, and publicly available metagenomes, revealing 178 dinoNAV EVEs, predominantly among hydrocoral-dinoflagellate metagenomes. Putative associations between Symbiodiniaceae and dinoNAV EVEs were corroborated by the characterization of dinoNAV-like sequences in 17 of 18 scaffold-scale and one chromosome-scale dinoflagellate genome assembly, flanked by characteristically cellular sequences and in proximity to retroelements, suggesting potential mechanisms of integration. EVEs were not detected in dinoflagellate-free (aposymbiotic) cnidarian genome assemblies, including stony corals, hydrocorals, jellyfish, or seawater. The pervasive nature of dinoNAV EVEs within dinoflagellate genomes (especially *Symbiodinium*), as well as their inconsistent within-genome distribution and fragmented nature, suggest ancestral or recurrent integration of this virus with variable conservation. Broadly, these findings illustrate how +ssRNA viruses may obscure their genomes as members of nested symbioses, with implications for host evolution, exaptation, and immunity in the context of reef health and disease.

**E**ndogenous viral elements, or “EVEs,” arise when whole or fragmented viral genomes are incorporated into host cell germlines. Once integrated, EVEs may propagate across successive host generations, potentially becoming fixed in a population through natural selection or drift<sup>1,2</sup>. Therefore, the presence and content of EVEs can provide clues into the evolutionary relationships among host species and shed light on ancient and modern virus-host interactions<sup>3</sup>. To date, most EVEs described in metazoan and plant genomes are retroviral, as this viral group must integrate their genome (as a provirus) into the genome of the host to replicate. Retroviruses thus possess and encode all of the molecular machinery (e.g. reverse transcriptases, integrases) required to integrate autonomously<sup>4</sup>. Remarkably, however, sequences from viruses that do not encode reverse transcriptases or exploit integration as a component of an obligate replication strategy—even viruses with no DNA stage—have also recently been detected as EVEs in diverse eukaryotic genomes<sup>5–11</sup>. These non-retroviral RNA EVEs have been reported in hosts ranging from unicellular algae to chiropteran (bat) genomes<sup>12–18</sup>. Though the mechanisms behind non-retroviral integration continue to be explored, viral sequences may be introduced via nonhomologous recombination and repair, through interactions with host-provisioned integrases and reverse transcriptases supplied on mobile elements (e.g. retroelements), or by utilizing co-infecting viruses<sup>6,7</sup>.

Endogenization of any viral sequence (including non-retroviral EVEs) may have positive, neutral or negative effects on a host<sup>19–21</sup>. While many EVEs are functionally defective or deleterious and ultimately removed from a population via purifying selection, retained EVEs may remodel the genomic architecture of their hosts or introduce sources of genetic innovation later co-opted for host function (i.e. exaptation<sup>22,23</sup>). Such ‘domesticated’ EVEs can be co-opted by hosts and utilized as regulatory elements, transcription factors, or functional proteins with purposes ranging from organism development to synaptic plasticity in the mammalian brain<sup>24–28</sup>. In particular, non-retroviral EVEs potentially serve as antiviral prototypes that help hosts combat infection by exogenous viruses currently circulating in the population<sup>14,29–31</sup>. Mechanisms underpinning EVE-derived immunity can include cell receptor interference, nucleic acid sequence recognition (e.g., RNAi), or even replication sabotage through production of faulty virus proteins from EVEs<sup>32</sup>. If expressed, EVEs may have a significant influence on the health, physiology and/or behavior of their hosts in natural and experimental systems<sup>31,33,34</sup>.

Investigating the distribution, sequence identity, and function of EVEs can yield insight into virus-host interactions across generations. EVEs catalogue a subset of the viruses that a host lineage has encountered and can link homologous extant viruses to contemporary hosts or known disease states<sup>31</sup>. Because integrated elements may accrue mutations at a slower rate than exogenous viral genomes<sup>6,35</sup>, EVEs can fill gaps in virus-host networks and act as synapomorphies, indicating the minimum time that a virus may have interacted with a host. As ‘genomic fossils’, EVEs have helped paleovirologists date the minimum origin of *Circoviridae*<sup>36</sup>, *Hepadnaviridae*<sup>37</sup>, *Bornaviridae*<sup>38</sup>, *Flaviviridae*<sup>39</sup>, *Lentiviridae*<sup>40,41</sup>, and *Spumaviridae*<sup>42</sup> infections within metazoans<sup>2,24,35,43,44</sup> (reviewed by Barreat and Katzourakis in 2022<sup>45</sup>).

Coral holobionts – the cnidarian animal and its resident microbial assemblage, including dinoflagellates in the family Symbiodiniaceae, bacteria, archaea, fungi, and viruses – are an ecologically and economically valuable, multipartite non-model system<sup>46,47</sup>. Symbiodiniaceae are key obligate nutritional symbionts of corals and support their hosts in the construction of reef frameworks<sup>48</sup>. However, environmental stress can break down

coral-Symbiodiniaceae partnerships, resulting in bleaching – the mass loss of Symbiodiniaceae cells<sup>49</sup>. Some bleaching signs (paling of a coral colony) are hypothesized to also result from viral lysis of Symbiodiniaceae<sup>21,50–54</sup>, but direct evidence supporting this hypothesis remains limited. Overall, the role of viruses in coral colony health and disease requires further examination.

Non-retroviral +ssRNA dinoRNAV sequences were first reported in stony corals based on five metatranscriptomic sequences and corroborated by Symbiodiniaceae EST libraries<sup>55</sup>. Subsequent studies indicated that similar +ssRNA viruses are commonly detected in coral RNA viromes and metatranscriptomes, as well as via targeted amplicon assays<sup>54,56–58</sup>. These viruses exhibit synteny and significant homology to *Heterocapsa circularisquama* RNA virus (HcRNAV<sup>57</sup>), the sole recognized representative of the genus *Dinornavirus* and a known pathogen of free-living dinoflagellates<sup>59</sup>. Both HcRNAV and dinoRNAV sequences detected in coral holobiont tissues contain two ORFs – a Major Capsid Protein (*MCP*) and RNA dependent RNA polymerase (*RdRp*). Furthermore, icosahedral virus-like particle (VLP) arrays resembling HcRNAV (but with 40% smaller individual particle diameters) have been imaged in the Symbiodiniaceae-dense coral gastrodermis tissue and in Symbiodiniaceae themselves<sup>60</sup>. Levin et al. (2017)<sup>57</sup> assembled the 5.2 kb genome of a putative dinoRNAV from a poly(A)-selected metatranscriptome generated from cultured *Symbiodinium*. The assembly contained a 5' dinoflagellate spliced leader (“dinoSL”<sup>61</sup>) – a component of >95% of Symbiodiniaceae mRNAs, speculated to illustrate molecular mimicry – and exhibited >1000-fold higher expression in a thermosensitive *Cladocodium* C1 population relative to a thermotolerant population of this Symbiodiniaceae strain at ambient temperatures (27 °C<sup>48,57</sup>). Together, the findings from these studies suggest that Symbiodiniaceae are target hosts of reef-associated dinoRNAVs.

This study (1) systematically searched for putative endogenized dinoRNAVs in metagenomes from in situ (symbiotic) coral colonies and seawater, as well as in available genomes of Symbiodiniaceae and aposymbiotic (symbiont-free) cnidarians, (2) investigated the evolutionary relationship of putative dinoRNAV EVEs to exogenous reef-associated dinoRNAV sequences, and (3) made preliminary inferences regarding the distribution and possible function of these dinoRNAV EVEs based on their detection, prevalence, and genomic context.

## Results and discussion

**Evidence of endogenized dinoRNAVs in coral holobiont metagenomes.** Putative dinoRNAV EVEs were detected in metagenomes generated from 42 cnidarian holobionts out of 269 sampled across the South Pacific Ocean (Supplementary Data 1). The majority of endogenized dinoRNAVs were identified in hydrocoral metagenomes (*Millepora* spp.; 70.5%, *n* = 105) which predominantly harbored *Symbiodinium* dinoflagellates but EVE-like sequences were also observed in scleractinian coral metagenomes (*Pocillopora* spp.; 29.5%, *n* = 15) which predominantly harbored *Cladocodium* and *Durusdinum* dinoflagellates (Fig. 1a, c). No dinoRNAV-like sequences were detected among *Porites* spp. metagenomes (Figs. 1, 2). Hydrocoral metagenomes were sequenced at equivalent depths as scleractinian corals and had comparable levels of annotation (Supplementary Fig. 1, Supplementary Data 2); thus, higher dinoRNAV EVE prevalence in hydrocoral libraries was likely not a result of methodological bias. Of the 11 evaluated South Pacific islands, dinoRNAV EVEs were identified in samples from eight (Guam, Gambier, Moorea, Cook, Niue, Malpelo, Coiba, and Las Perlas), spanning 18 unique sites (Fig. 1b, d). Among *Pocillopora* spp. metagenomes, putative dinoRNAV EVEs were only

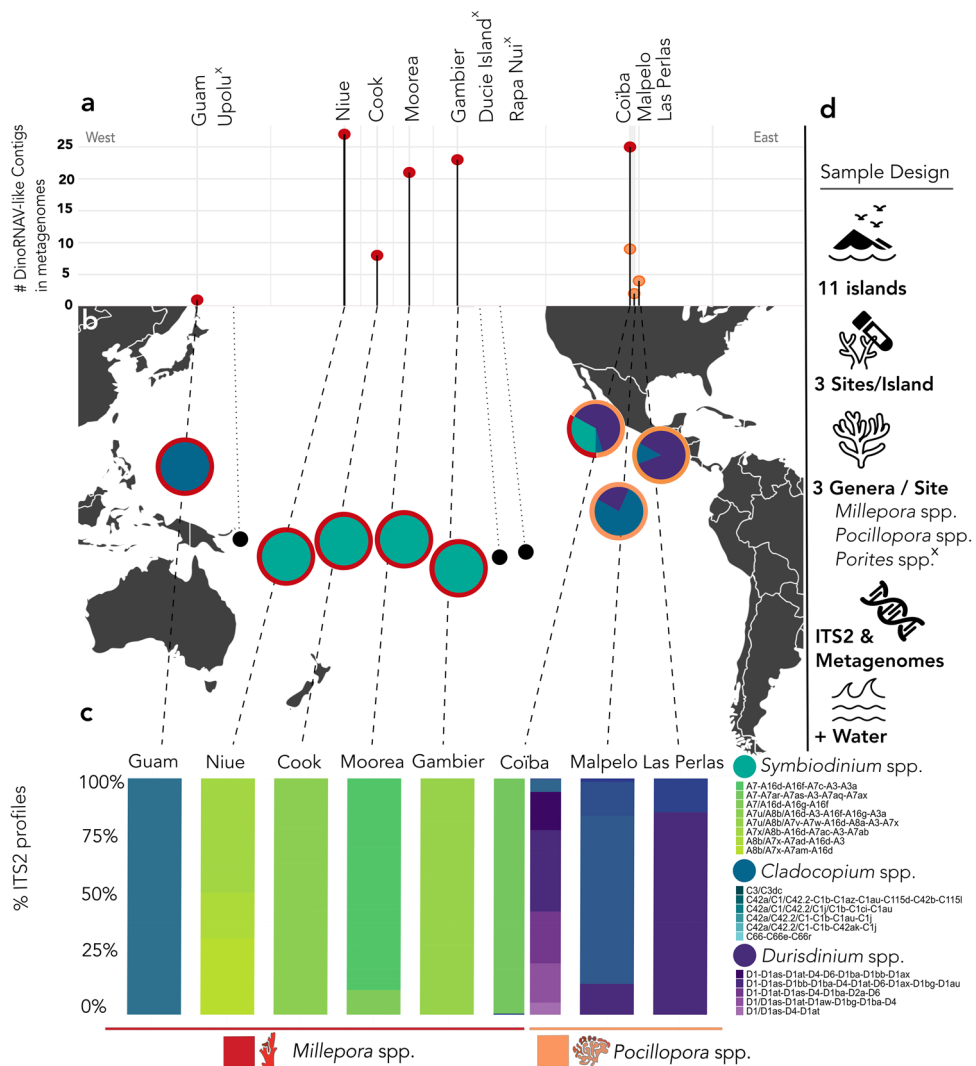


**Fig. 1 Islands and species (cnidarian and dinoflagellate) correlating with dinoRNAV EVE-like sequence detection among Tara Pacific metagenomes.**

**a** Count of scaffolds with putative endogenized dinoRNAV-like sequences among Tara Pacific metagenomes, grouped by island and spaced longitudinally by location sampled. **b** Sampling sites of Tara Pacific metagenomes explored for endogenized dinoRNAV-like sequences in this study. Internal circles indicate dominant Symbiodiniaceae genera based on ITS2 type profiles, outer ring denotes coral host(s) sampled at each island. **c** Symbiodiniaceae ITS2 type profile metabarcoding as delineated via Symportal<sup>119</sup> within island and host. **d** Sample design of Tara Pacific libraries queried for dinoRNAV EVEs. [x] and black circles on map indicate island locations or species where no dinoRNAV-like sequences were detected. Icons derived from the Noun Project.

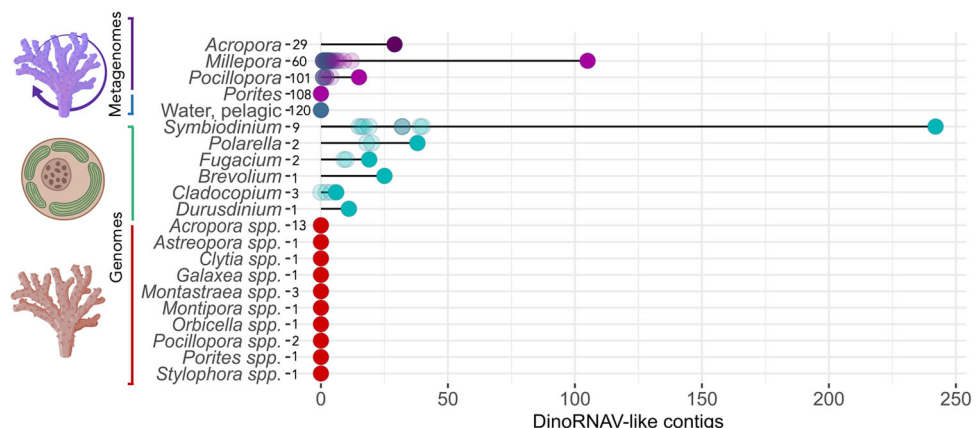


**Fig. 2 Quantity of putative endogenized dinoRNAV per metagenome or genome.** Total quantity of putative endogenized dinoRNAV EVEs identified, broadly organized by sample source (metagenome or genome), and number of libraries or assemblies queried (after source name, Supplementary Data 6). Opaque circles denote the sum total of dinoRNAV EVE-like sequences identified from each source, while transparent circles denote individual counts of putative dinoRNAV EVEs per library. Icons created with BioRender.

identified on the Central American coast (CAMR, Coastal Pacific Longhurst Province) and were absent in Melanesia, Micronesia, and Polynesia; at these latter sites, dinoRNAVs were largely found in *Millepora* hydrocoral metagenomes. Importantly, endogenized dinoRNAV open reading frames (ORFs) appeared to be immediately adjacent to ORFs identified as dinoflagellate (typically Symbiodiniaceae) genes—they were not proximal to coral genes or those of other cellular organisms abundant in these metagenomes (Supplementary Data 3).

We examined the Symbiodiniaceae ITS2 profiles associated with each metagenome and found that putative dinoRNAV EVEs were primarily associated with *Symbiodinium*, *Cladocopium*, and *Durusdinum*, which exhibited variation on both host and regional scales (Fig. 1c, Supplementary Data 4). DinoRNAV EVEs were more common in *Symbiodinium*-dominated cnidarians ( $F_{2,1044} = 25.8$ ,  $p < 0.0001$ , nested ANOVA; Supplementary Fig. 2, Supplementary Data 5) relative to cnidarians hosting other Symbiodiniaceae genera, regardless of host. This suggested that dinoRNAV integration may be particularly recurrent or conserved within the genus *Symbiodinium* (Fig. 1).

To determine if these putative viral integrations were specific to cnidarian holobiont metagenomes and ensure that they were not artifacts of shared sample processing and sequencing procedures of the Tara Pacific pipeline, we also analyzed seawater metagenomes and publicly available metagenomes from the stony coral-dinoflagellate holobiont, *Acropora* spp. (Supplementary Data 1B, <sup>62–69</sup>). Examination of 120 Tara Oceans pelagic seawater metagenomes<sup>70</sup> yielded no sequences sharing homology to dinoRNAVs. The concentration of Symbiodiniaceae cells within cnidarian tissues is considerably higher than that of the surrounding seawater<sup>71–74</sup>. On average, only  $1.46 \pm 0.08\%$  of assembled contigs in seawater metagenomes were annotated as Symbiodiniaceae. Thus, lack of detection of dinoRNAV-like sequences from seawater metagenomes is likely due to reduced genomic signal of Symbiodiniaceae in the water column, rather than a lack of EVEs associated with Symbiodiniaceae lineages in seawater. However, it also must be noted that these Tara Oceans seawater metagenomes were not collected concurrently with coral samples<sup>75</sup>. Analysis of the 30 non-Tara *Acropora* holobiont metagenomes identified 29 more putative dinoRNAV EVEs (Fig. 2; Supplementary Data 6). These dinoRNAV EVEs were again neighboring dinoflagellate ORFs. While the Caribbean *Acropora* metagenomes analyzed contained too few reads to resolve the dominant Symbiodiniaceae present, earlier studies of the same coral colonies identified *Symbiodinium* spp. as the primary symbiont present<sup>76</sup>.

The identification of endogenized dinoRNAV-like sequences in cnidarian holobiont metagenomes, combined with the proximity of dinoRNAV-like ORFs to dinoflagellate-like sequences across metagenomes harboring diverse dinoflagellate consortia, collectively indicate that dinoRNAV EVEs are widespread among Symbiodiniaceae genera (Fig. 2 cyan dots).

**Endogenized DinoRNAVs detected in Symbiodiniaceae genomes.** To further test the hypothesis that dinoRNAVs on reefs infect dinoflagellate symbionts and not cnidarians, we examined 18 scaffold-scale genome assemblies representing the dinoflagellate families Symbiodiniaceae and Suessiaceae as well as 25 cnidarian genomes spanning 10 genera (Supplementary Data 1B<sup>62–69</sup>, Fig. 2; Table 1). Alignments revealed no evidence of endogenized dinoRNAVs in any of the 151,782 aposymbiotic (dinoflagellate-free) cnidarian scaffolds. In contrast, the same approach uncovered 351 (of 593,433) dinoflagellate scaffolds with evidence of endogenized dinoRNAVs (Fig. 2; Table 1). The identified 351 dinoRNAV EVE-containing scaffolds were

observed across 17 of the 18 dinoflagellate genome assemblies (Table 1). DinoRNAV EVEs were also observed in two assemblies from the free-living dinoflagellate genus, *Polarella* (family Suessiaceae), which is closely related to the family Symbiodiniaceae, and served as an outgroup in this study<sup>77,78</sup>. Interestingly, assemblies belonging to *Symbiodinium*, the most ancestral Symbiodiniaceae genus<sup>48</sup>, contained a higher number of scaffolds with putative dinoRNAV EVEs ( $\bar{x}=28.11$ ,  $stdev=10.7$ ) relative to assemblies of other Symbiodiniaceae genera ( $\bar{x}=8.71$ ,  $stdev=11$ ; Fig. 2 cyan dots; Table 1). This result may clarify why observations of dinoRNAV-like ORFs were more common in metagenomes dominated by *Symbiodinium* (Fig. 1c). The dinoflagellate genome assembly with no detected dinoRNAV EVEs belonged to a relatively incomplete assembly of *Cladocopium* C15, which had the second lowest N50 and lowest BUSCO completeness score of all genomes examined (completeness 11.6%, relative to the average 24.54%; Table 1, Supplementary Data 7). The lower coverage/completeness of the *Cladocopium* C15 assembly indicates a reduced window into this genome. It is therefore possible that when a more complete assembly is generated, dinoRNAV EVE-like sequences will be detectable from this dinoflagellate. However, a linear model suggested that there was no relationship between dinoRNAV EVE detection and assembly statistics (i.e. query length, N50, or completeness; see Supplementary Data 8 for linear model output). Instead, dinoflagellate genus was the strongest predictor of dinoRNAV detection in a genome (LM results: Genus  $F=5.74$ ,  $p=0.012$ ) and dinoRNAV detections were significantly higher in *Symbiodinium* than *Cladocopium* genomes (pairwise estimated difference =  $-27.77 \pm 5.91$ ,  $p=0.01$ ; Supplementary Data 9). Furthermore, since we were unable to detect dinoRNAV EVEs in *Porites* metagenomes—a coral species primarily harboring *Cladocopium* C15 symbionts—we hypothesize that dinoRNAV endogenization was either less common in this lineage of Symbiodiniaceae or integrations have been lost over evolutionary time<sup>79,80</sup>.

**Incomplete ORFs and possible duplications indicate endogenization of DinoRNAVs.** The repeated observation of putative dinoRNAV EVEs in dinoflagellate scaffolds and contigs from metagenomes and genomes suggests these sequences are either (1) conserved sequence artifacts of Symbiodiniaceae-dinoRNAV interactions, and/or (2) evidence of highly prevalent dinoflagellate viruses, commonly integrated and propagated via their single-celled hosts. If the observed dinoRNAV-like sequences represent active infections capable of generating virions during egress, we would, at minimum, expect essential ORFs associated with replication (RNA-dependent RNA polymerase, *RdRp*) and virion structure (Major Capsid Protein, *MCP*) to be endogenized on the same scaffold. We would additionally expect to observe overall conservation of ORF length/composition (with a lack of internal stop codons or substantial deletions) when aligning the dinoRNAV-like sequences detected here with known exogenous dinoRNAV sequences.

However, both DIAMOND and gene prediction analyses generally depicted dinoRNAV-like ORFs in isolation on separate scaffolds. While 28 *MCP* and 73 *RdRp* dinoRNAV ORFs were annotated, both ORFs were present on a Symbiodiniaceae scaffold – potentially representing whole dinoRNAV genome integrations – in only 14 instances. Thirteen of these 14 were from *Symbiodinium* genomes, whereas one scaffold was from *Breviolum minutum*, a member of the second most ancestral dinoflagellate genus (Table 1)<sup>48</sup>. To assess the conservation of putative dinoRNAV EVE sequence length/composition, we aligned the genomic and single ORF EVEs to reference exogenous dinoRNAV sequences. The reference genome for reef-associated dinoRNAVs is  $\sim 5$  Kbp

**Table 1** DinoRNAV EVE-like open reading frames from representative Symbiodiniaceae and Suessiaceae dinoflagellate scaffold-level genome assemblies.

Dinoflagellate Species (strain)	Total # Scaffolds	Host	Location	BUSCO score	dinoRNAV EVE ORFs on scaffolds		Both
					RdRp	MCP	
Symbiodiniaceae							
<i>Symbiodinium linucheae</i> (CCMP2436) <sup>83</sup>	37,772	<i>Plexaura homomalla</i>	Bermuda	21.8%	39	0	1
<i>Symbiodinium microadriaticum</i> (04-5035SCL03) <sup>83</sup>	57,558	<i>Orbicella faveolata</i>	Florida, USA	41.6%	30	1	3
<i>Symbiodinium microadriaticum</i> (CassKB8) <sup>83</sup>	67,937	<i>Cassiopea</i> sp.	Hawaii, USA	73.3%	29	1	3
<i>Symbiodinium microadriaticum</i> (CCMP2467) <sup>113</sup>	9688	<i>Sylophora pistillata</i>	Red Sea	15.6%	29	1	3
<i>Symbiodinium natans</i> (CCMP2548) <sup>83**</sup>	2855	N/A (Isolated from seawater)	Hawaii, USA	15.5%	14	1	3
<i>Symbiodinium necroappetens</i> (CCMP2469) <sup>83*</sup>	104,583	<i>Condylactis gigantea</i>	Jamaica	22.8%	37	4	2
<i>Symbiodinium pilosum</i> (CCMP2461) <sup>83**</sup>	48,302	<i>Zanthus sociatus</i>	Jamaica	19.8%	15	0	0
<i>Symbiodinium</i> sp. A5 (formerly S. tridacnidorum) <sup>83</sup>	6245	<i>Heliofungia actiniformis</i>	Australia	21.1%	17	1	0
<i>Symbiodinium tridacnidorum</i> (sh18 A3 Y106) <sup>114</sup>	16,176	<i>Tridacna crocea</i>	Japan	19.8%	20	1	0
<i>Brevilium minutum</i> (Mf105b) <sup>115</sup>	21,899	<i>Orbicella faveolata</i>	Florida, USA	14.2%	21	3	1
<i>Cladocodium</i> C15 <sup>116</sup>	34,589	<i>Porites lutea</i>	Australia	11.6%	0	0	0
<i>Cladocodium</i> sp. Clacro (formerly C. goreau) <sup>89</sup>	41,289	<i>Acropora tenuis</i>	Australia	27.7%	4	0	0
<i>Cladocodium</i> sp C92 (Y103) <sup>114</sup>	6686	<i>Fragum</i> sp.	Japan	19.5%	2	0	0
<i>Durusdinium trenchii</i> <sup>117</sup>	19,593	<i>Favia speciosa</i>	Japan	28.7%	10	1	0
<i>Fugacium kawagutii</i> (CS156 CCMP2468) <sup>89</sup>	16,959	N/A (Free-living)	Hawaii, USA	8.3%	8	1	0
<i>Fugacium kawagutii</i> (CCMP2468) <sup>118</sup>	30,040	N/A (Free-living)	Hawaii, USA	17.9%	9	1	0
<i>n</i> = 314 scaffolds with DinoRNAV EVE-like sequences							
Suessiaceae							
<i>Polarella glacialis</i> (CCMP1383) <sup>78**</sup>	33,494	N/A (Free-living, isolated from seawater)	Antarctica	20.8%	20	0	0
<i>Polarella glacialis</i> (CCMP2088) <sup>78**</sup>	37,768	N/A (Free-living, isolated from seawater)	Arctic	21.8%	18	0	0
<i>n</i> = 38 total scaffolds with DinoRNAV EVE-like sequences							

Total counts of dinoflagellate scaffolds in genomes queried with individual endogenized dinoRNAV ORFs (RdRp, MCP) or both nearby each other, potentially indicating full viral genome integration. Table supplies associated dinoflagellate host species and location of isolation. RdRp = RNA-dependent RNA polymerase; MCP = major capsid protein 1 assembly coverage and completeness are measured via BUSCO score (% completeness or %C)<sup>102</sup>. \* indicates species with documented opportunistic life history. \*\* indicates species with documented free-living life history per principal species description. Gonzalez-Pech et al.<sup>114</sup>, Aranda et al.<sup>83</sup>, Shoguchi et al.<sup>117</sup>, Lin et al.<sup>118</sup>, Shoguchi et al.<sup>119</sup>, Liu et al.<sup>116</sup>, Robbins et al.<sup>115</sup>, Shoguchi et al.<sup>117</sup>, Stephens et al.<sup>78</sup>. Further genome citations (including accession numbers) and BUSCO completion metrics can be found in Supplementary Data 7 and in superscript.

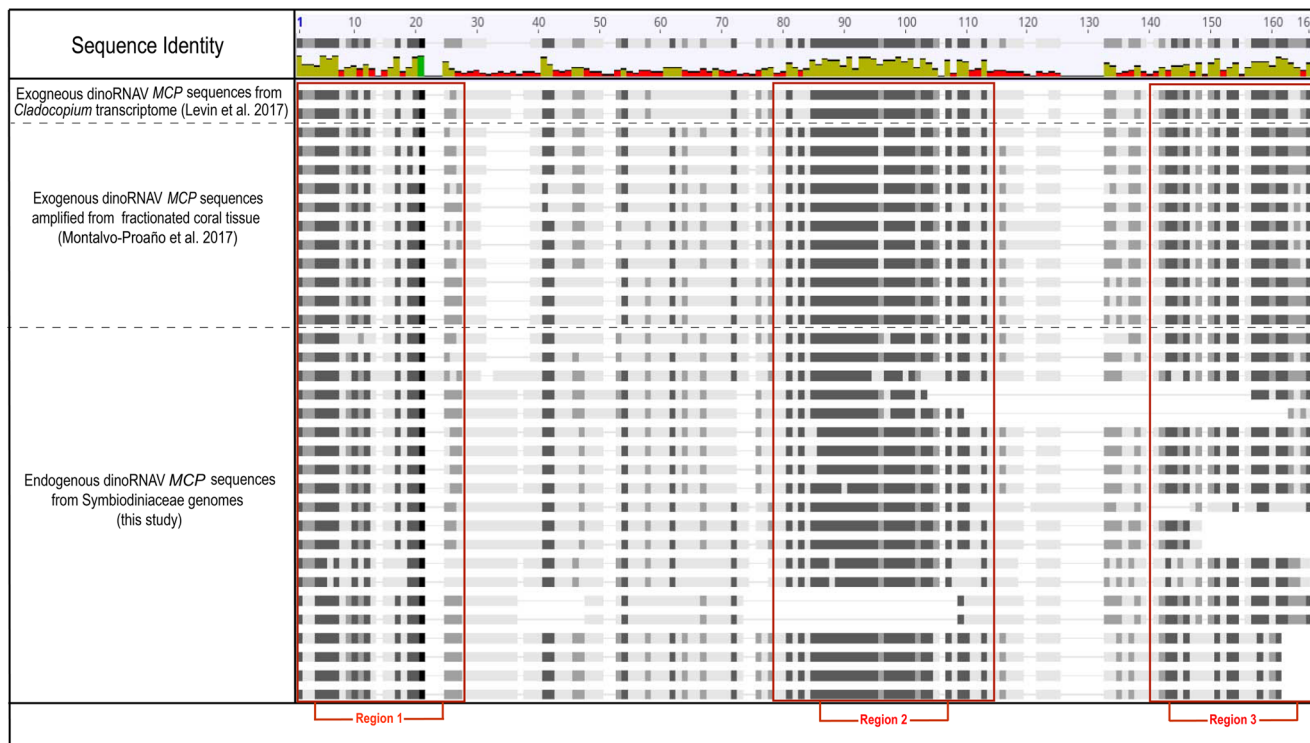


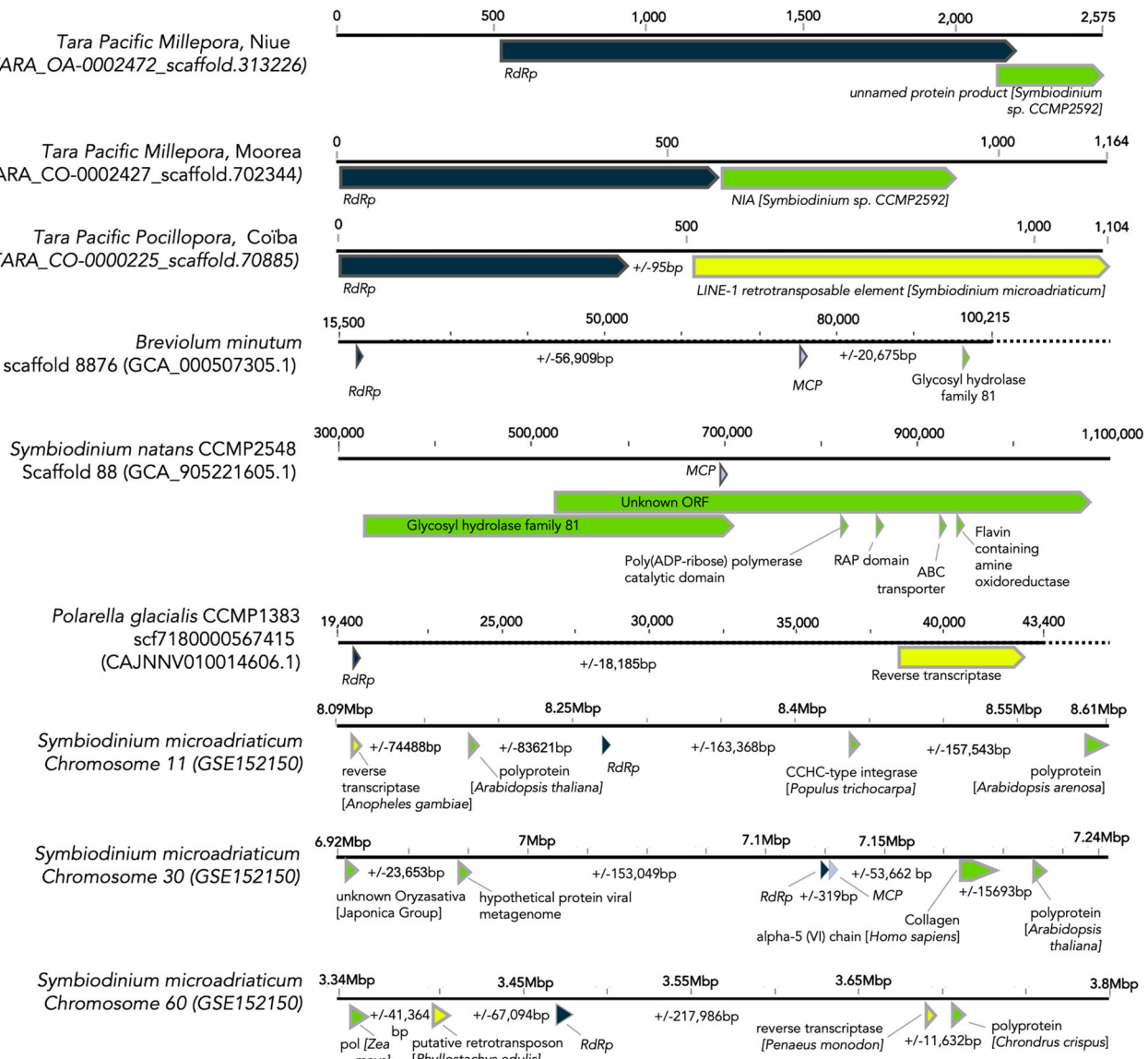
**Fig. 3 Amino acid alignment of putative endogenous and exogenous dinoRNAV-like +ssRNA virus Major Capsid Protein (MCP) sequences against transcriptome reference.** Putatively endogenous dinoRNAV Major Capsid Protein (MCP) amino acid sequences were aligned against exogenous references, including: (1) Symbiodiniaceae +ssRNA virus MCP ORFs recovered from a *Cladocopium* sp. transcriptome (Levin et al. 2017), and (2) dinoRNAV MCP amplicons from fractionated coral tissue (Montalvo-Proaño et al. 2017). Conserved regions were observed between exogenous and putatively endogenous viral sequences (labeled Regions 1–3).

long and contains a 1,071 bp noncoding region between ORFs, with a 124-nucleotide internal ribosomal binding site<sup>57</sup>. In this study, for 13 of the scaffolds in which dinoRNAV ORFs were detected, the putative noncoding region between the *MCP* and *RdRp* EVEs ranged from ~200–800 bp (except for a scaffold belonging to *S. linucheae* CCMP2456, which contained a ~79 kbp noncoding region, and was excluded in further alignments). No internal ribosomal binding sites were detected within the putative dinoRNAV EVEs identified in dinoflagellate genomes. A nucleotide-based alignment to Levin et al.'s (2017)<sup>57</sup> reference dinoRNAV genome indicated that the putative dinoRNAV EVEs presented here contained substantial insertions and/or deletions (Supplementary Fig. 3). Translated exogenous dinoRNAV MCP ORFs are reported to be ~358 aa in length<sup>57</sup>; Fig. 3 top sequences), but dinoRNAV-like MCP sequences recovered in this study ranged from 116–605aa in length. Furthermore, comparisons of these endogenous MCPs to exogenous reference sequences revealed internal stop codons and overall low similarity (Fig. 3). Amino acid-based alignment of endogenous dinoRNAV MCPs to metatranscriptome- and amplicon-generated exogenous reference sequences<sup>57,58</sup> revealed indels and regions of low similarity between three conserved regions across both endogenous and exogenous MCP sequences (red boxes in Fig. 3).

Interestingly, multiple whole dinoRNAV integrations were sometimes observed in a single dinoflagellate genome. For example, genome assemblies of four different *S. microadriaticum* strains contained two or three whole dinoRNAV EVEs each (Table 1; Fig. 2). Pairwise alignments measuring shared nucleotide identity of whole dinoRNAV EVEs across Symbiodiniaceae scaffolds revealed that the *S. microadriaticum* genomes and the *S. necroappetens* genome share two whole genome dinoRNAV EVEs (provisionally dinoRNAV-A and dinoRNAV-

B; Supplementary Fig. 3; Clustal-Omega)<sup>81</sup>. *S. microadriaticum* dinoRNAV-B was identical in all strains and shared 97% identity with the *S. necroappetens* dinoRNAV-B, yet proximal genes varied (Supplementary Data 10, 11). Importantly, the inconsistent composition and fragmented nature of both the genomic and single ORF dinoRNAV EVEs reported here supports the hypothesis that these sequences are not capable of generating replicative virions and are best interpreted as multiple integrations of dinoRNAVs into a host genome.

**A Potential Mechanism for dinoRNAV Endogenization: Host-Provisioned Retroelements.** To assess if general genomic “neighborhoods” are conserved across dinoRNAV integrations (e.g. site location and synteny) and to better understand the genes proximal to EVEs on Symbiodiniaceae genomes, a chromosome-scale *Symbiodinium microadriaticum* genome assembly was evaluated (Fig. 4). The highest quality dinoflagellate genome assembly currently available revealed dinoRNAV-like ORFs on 18 of 94 chromosomes, with at least one *RdRp* on each, and some with multiple (two with  $n = 2$  *RdRps*, three with  $n = 3$  *RdRps*). On three of the chromosomes (# 30, 35, and 74), there were predicted ORFs annotated as dinoRNAV *MCPs* in close proximity to a *RdRp* ORF (separated by noncoding regions 319–656nt), indicative of a potential full-length dinoRNAV genome integration. These results corroborate detections of multiple genomic dinoRNAV EVEs in scaffold-scale assemblies of *Symbiodinium microadriaticum* genomes (Supplementary Fig. 3). The higher-resolution *S. microadriaticum* chromosome-level assembly facilitated the identification of an additional dinoRNAV genomic EVE ( $n = 4$  for chromosome-level vs.  $n = 3$  for scaffold-level, Supplementary Fig. 3), two of which were identified on Chromosome 74 and were separated by 2501 nucleotides. Of note,



#### Open Reading Frame Annotations

- RNA dependent RNA polymerase (RdRP)
- Putative Cellular/Dinoflagellate ORF
- Major Capsid Protein (MCP)
- Putative RT/Transposon Cellular ORF

**Fig. 4 Representative scaffolds and chromosome fragments containing putative dinoRNAV EVEs.** Scaffolds annotation: MCP ORFs are indicated by light blue, RdRp indicated by navy blue ORFs (with complete description in Supplementary Data 10). Open reading frame (ORF) color broadly indicates cellular versus putative +ssRNA viral homology; yellow and some green (e.g., integrases, polyproteins) ORFs may be exploited mechanisms for viral integration. (+/-) base pair values represent sequence lengths between ORFs.

Nand et al. (2021)<sup>82</sup> reported a decreasing abundance and expression of genes towards the center of chromosomes (past ~2Mpb of a telomere), where there was an increase in repetitive elements; this is where 26 of 29 putative dinoRNAV EVEs were identified in the chromosome-level assembly. Furthermore, ORFs neighboring integrations often varied widely, both in proximity and predicted function, from collagen and RNA binding protein to reverse transcriptase and non-LTR retrotransposable elements. These ORFs potentially contributed to the endogenization of dinoRNAV via mechanisms such as retrotransposition (Fig. 4, Supplementary Data 10).

Retroposition through host-provisioned retroelements is one proposed mechanism of non-retroviral RNA virus integration into eukaryotic genomes<sup>6,7</sup>. An indicator of this form of integration is the nearby presence of a relict dinoflagellate spliced

leader (“dinoSL”), a 22nt sequence located at the 5’ end of mRNAs<sup>83–86</sup>. Such a sequence flanks the RdRp gene on some extant dinoRNAVs<sup>57</sup>. We detected dinoSLs within 500 bp of 23.1% (six of 26) endogenized RdRp ORFs on *S. microadriaticum* chromosomes, providing support for retroposition of these viral elements into Symbiodiniaceae genomes (Supplementary Data 11, 12). DinoRNAV gene integration may be facilitated by any of three major orders of retroelements associated with Symbiodiniaceae, including long terminal repeat (LTR) retrotransposons, short interspersed nuclear elements (SINEs), and long interspersed nuclear elements (LINEs<sup>83,87,88</sup>). Evidence suggests that these LINEs are common and non-active remnants of an ancient proliferation of LINEs that preceded the diversification of *Suessiales*<sup>78,83,89</sup>. *Symbiodinium* contains more LINEs relative to other Symbiodiniaceae genera, comprising 74.10–171.31 Mbp of

*Symbiodinium* genomes, relative to an average of 7.48 Mbp of the genomes of in other genera, indicating the loss of these retroelements across speciation events<sup>82,83</sup>. The loss of LINEs in more recently derived Symbiodiniaceae genera coincides with a decrease in dinoNAV EVE detection in these genomes (Table 1). Conversely, the genomes of *Polarella*, the psychrophilic and free-living outgroup from which Symbiodiniaceae diversified ~160 million years ago, are LINE-rich and generally have comparable numbers of dinoNAV EVEs to *Symbiodinium* (Table 1<sup>48,77,78,83</sup>). Together, this suggests that LINE activity during speciation may have facilitated dinoNAV integration and the resulting EVEs may constitute dinornavirus “fossils.” This may explain their degree of sequence fragmentation and relatively low sequence similarity to modern extant dinoRNAs (Fig. 3).

LINE-mediated retroposition is further supported by the observation of a LINE reverse transcriptase homolog ~17 kbp upstream of a *RdRp* EVE with a relict dinoSL on chromosome 45 (Supplementary Data 12) and a LINE retroelement 95 bp downstream of an EVE recovered from a *Pocillopora* metagenome (Fig. 4). Additionally, ~40% of annotated ORFs (35 of 88 annotated proteins) proximal to dinoNAV ORFs on *S. microadriaticum* chromosomes were similar to non-LTR elements seen in other eukaryotic genomes sometimes <300 bp 5' upstream (Supplementary Data 12, Supplementary Fig. 4). Collectively, these findings implicate host provisioned retroelements, such as LINEs, as facilitators of dinoNAV gene integration.

#### DinoNAV EVEs show homology to extant exogenous viruses.

Modern, exogenous dinoRNAs (Order: *Sobelivirales*) are highly divergent and hypothesized to form chronic infections within dinoflagellate hosts<sup>54,55,57,58</sup>. This chronic infection strategy likely provides opportunities for retroelement-driven endogenization into host genomes. Because many EVEs evolve at the rate of the host genome, rather than at the much faster rate of exogenous +ssRNA viral genomes, EVEs can serve as a snapshot of viral ancestry<sup>90</sup>. We compared translated dinoNAV EVEs to exogenous dinoRNAs and other *Dinornavirus* taxa to assess the conservation of EVEs, the potential for host utilization of these elements, and their relatedness to contemporary dinoRNAs. We found that amino acid translations of endogenous dinoNAV MCP sequences contained conserved motifs observed in the exogenous MCP sequences (e.g. Regions 1–3 in Fig. 3), yet the associated phylogeny was highly polyphyletic along inferred ancestral nodes (Fig. 5a). Endogenous MCP ORFs also appear to be evolving under neutral selection (dN/dS=0.958).

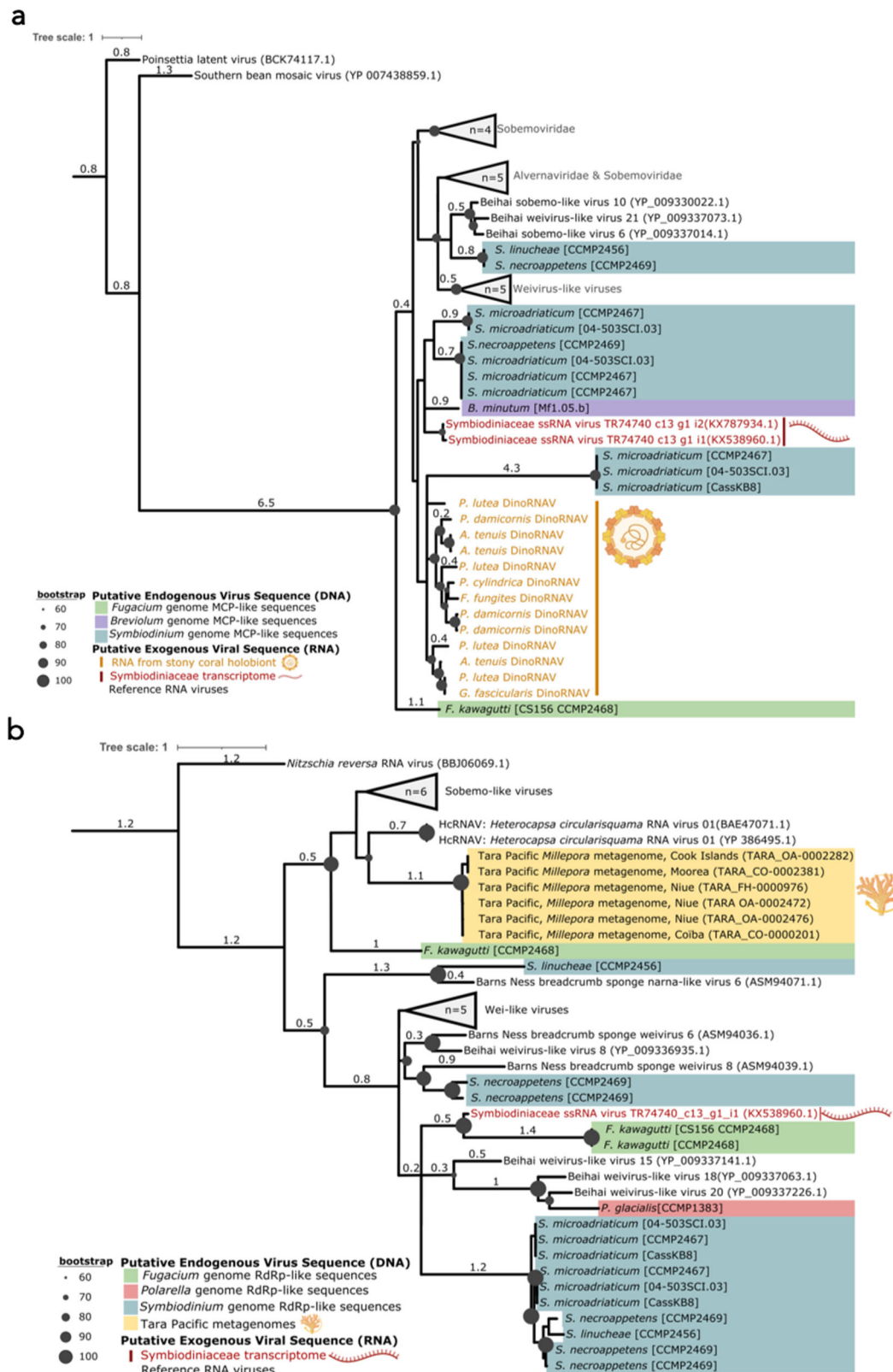
Endogenized dinoNAV MCP form their own clades within the MCP tree, each closely related to specific clades consisting of extant dinoRNAs or environmental (i.e. unclassified) sobeliviruses with similar conserved motifs. The majority of dinoNAV MCP EVEs shared similarity to extant MCPs identified from unfractionated stony coral holobionts via amplicon sequencing<sup>58</sup>; these sequences formed an independent, disorganized clade (Fig. 5a clade containing yellow and blue sequences), relative to those recovered from dinoflagellate transcriptomes or those of other invertebrate hosts. Likewise, dinoNAV *RdRp* EVEs identified via metagenomics appear most similar to HcNAV, the defining member of family Alvernaviridae and a protist pathogen, further supporting the affiliation of this EVE with a dinoflagellate host. MCP and *RdRp* ORFs putatively derived from the same dinoflagellate genomes often shared clades (clades containing multiple blue or green sequences in Fig. 5a, b), perhaps indicative of duplications within genomes or multiple integration events of particular dinoNAV lineages within host genera. The detection of putative dinoNAV *RdRp* ORFs within *Polarella* genomes is therefore indicative of either the antiquity of dinoNAV-dinoflagellate interactions and/or a propensity for recent dinoNAV integration across Dinophyceae families. However, the

exclusion of the *P. glacialis* dinoNAV-*RdRp* from *RdRps* of other dinoflagellate clades (pink, Fig. 5B) further illustrates the congruence between EVEs and their host genomes. Overall, the evident homology to contemporary *Dinornaviruses* support these integrations as Alvernaviridae within order *Sobelivirales*.

The expression and functional potential of endogenized dinoNAV elements (if any) remains unclear. With no isolated Symbiodiniaceae-infected dinoNAV strains available, investigation into EVE functionality is limited to *in silico* approaches. Sequence data mining efforts identified RNA sequences either sharing sequence similarity with dinoRNAs, or containing whole dinoNAV-like ORFs that also annotated as dinoflagellate transcripts (i.e. with cellular ORFs or sequence similarity) in seven out of nine publicly accessible dinoflagellate transcriptomes (Supplementary Data 13). Additionally, two transcripts from an exogenous dinoNAV infection identified in *Cladocopium* transcriptomes carried MCP ORFs of +ssRNA viral sequences ('TR74740\_c13-g1\_i1' and 'TR74740\_c13-g1\_i2'<sup>57</sup>, red text in Fig. 5a) and form a clade with putative *Symbiodinium* dinoNAV EVEs (Fig. 5). Likewise, the *RdRp* ORF of 'TR74740\_c13-g1\_i1' and the *RdRp* of 'GAKY01194223.1'—a transcript derived from a cultured *Symbiodinium microadriaticum* A1 transcriptome—shared some areas of similarity to putative endogenous dinoRNAs (Fig. 5b<sup>57,91</sup>). Importantly, both RNA transcripts also shared features characteristic of dinoflagellates, such as a 5' dinoSL<sup>61</sup> or dinoflagellate sequence space flanking the dinoNAV itself<sup>91</sup>. Furthermore, 'TR74740\_c13-g1\_i1' appeared to be in the top 0.03% of expressed transcripts at under certain thermal conditions, and GAKY01194223.1 appeared to exhibit moderately differential expression at the extremes of temperature and ionic stress in a cultured host<sup>57,91</sup>.

While viral *RdRps* have been leveraged by eukaryotes in multiple pathways<sup>92</sup>, the apparent fragmentation of the putative dinoNAV EVEs in *silico* may indicate a role in triggering antiviral mechanisms within their hosts<sup>31,93</sup>. Given that the *Symbiodinium* genome contains all core RNAi protein machinery, including Argonaute and Dicer, and that GAKY01194223.1 folds into several hairpins ( $\Delta G = -142.5$  kcal/mol; Supplementary Fig. 5 examples), Symbiodiniaceae may use the putative EVE ncRNA identified here to develop host immunity against extant, exogenous dinoRNAs. Furthermore, Symbiodiniaceae harboring dinoNAV EVEs also contained numerous non-retroviral EVEs of other viral families (Supplementary Data 11, Fig. 7) in close proximity, such as *Herpesviridae*, *Baculoviridae*, *Poxviridae*, *Iridoviridae*, *Phycodnaviridae*, *Pandoraviridae* and *Pithoviridae*, ssDNA viruses of the family *Shotokuvirae*, -ssRNA viruses from the family *Rhabdoviridae* and +ssRNA viruses from the family *Coronaviridae* (Supplementary Fig. 6). Metagenomes corroborate findings of similar *RdRps* from these viral families (Supplementary Fig. 6). This provides support for host-mediated integration (e.g. retroposition) as a means of defense for single celled organisms, though further research is needed<sup>94</sup>.

**Conclusions.** Over recent decades, endogenous viral elements (EVEs) have enabled investigators to better understand the evolutionary history of viruses (“paleoviology”) in diverse terrestrial systems, uncovering ancient and modern virus-host interactions. Our study further demonstrates how *in silico* identification of EVEs can provide ecological context for enigmatic viral genomes in non-model, multipartite systems such as coral holobionts, impacting how we study coral reefs and their viral consortia. Here, we detected heritable integrations of multiple putative dinoNAV genes in Symbiodiniaceae scaffolds from cnidarian metagenomes, as well as in diverse genomes of cultured Symbiodiniaceae; no integrations were detected from seawater metagenomes nor diverse aposymbiotic cnidarian genomes. The



apparent pervasive nature of dinoRNAV-like sequences among dinoflagellate genomes (especially the genus *Symbiodinium*) suggests widespread and recurrent/ancestral integration of these EVEs. We propose that host-provisioned mechanisms drive dinoRNAV integration into single-celled dinoflagellate genomes as EVEs. The findings presented in this study further validate the dinoRNAV-Symbiodiniaceae virus-host pair, enhancing our

understanding of ecologically and economically important cnidarian holobionts and opening the door to examining the role of EVEs in reef health.

## Methods

**Identification and computational validation of dinoRNAV EVEs leveraging meta'omics.** The Tara Pacific Expedition (2016-2018) sampled coral reefs to

**Fig. 5 Phylogenies of dinoNAV major capsid protein (MCP) and RNA-dependent RNA polymerase (RdRp) ORFs.** **a** dinoNAV Major Capsid Protein (MCP) ORF phylogeny. Maximum-likelihood tree of MCP amino acid sequences generated with a LG + F + G4 substitution model and 50,000 parametric bootstraps, illustrating the similarity of putative dinoNAV EVEs (this study) to extant dinoNAVs from stony coral colonies. **b** RNA-dependent RNA polymerase (RdRp) ORF phylogeny. Maximum-likelihood tree of RdRp amino acid sequences generated with a Blosum62 + G4 substitution model and 50,000 parametric bootstraps, demonstrating the similarity of metagenomic dinoNAV EVE RdRPs to RdRPs of the sole recognized *Dinornavirus*, *Heterocapsa circularisquama* RNA virus (HcRNAV), as well as alignment to each other. ORFs were recovered from host metagenomes, transcriptomes, genomes, and extant +ssRNA reference viruses from amplicon libraries (a only). Both trees include *Dinornavirus* reference sequences and visualized in iTOL.

investigate reef health and ecology using multiple methods, including amplicon sequencing and metagenomics (see Pesant et al. 2020<sup>95</sup> and <https://doi.org/10.5281/zenodo.4068293> for coral reef sampling and processing methods). In this study, we explored metagenomes generated from hydrocorals ( $n = 60$  *Millepora*), stony corals ( $n = 108$  *Porites*,  $n = 101$  *Pocillopora*) sampled from 11 islands (three replicate sites per island) across the South Pacific Ocean during the Tara Pacific Expedition for dinoNAV EVEs (Fig. 1, Supplementary Data 1A, 1B<sup>95</sup>). Amplicon libraries of the dinoflagellate Internal Transcribed Spacer 2 (ITS2) gene fragment were sequenced in tandem with the metagenomes, to characterize the dominant Symbiodiniaceae harbored by hydrozoan and stony coral colonies<sup>95</sup>.

To confirm that these dinoNAV EVE sequences were affiliated with coral holobionts and reduce the possibility that they are technical artifacts, publicly available metagenome libraries were analyzed (Supplementary Data 1B). These additional libraries included 120 assembled pelagic water samples presumed to include pelagic dinoflagellate sequences from the Tara Oceans dataset (2009–2013<sup>70</sup>) and 30 MiSeq metagenomes from unfractionated samples of the stony coral genus *Acropora*, which were processed and sequenced via a different pipeline (Supplementary Data 1B, Supplementary Fig. 7). Publicly accessible transcriptomes from nine Symbiodiniaceae assemblies (Supplementary Data 1B) were also queried to determine if dinoNAV-like sequences were present in poly(A)-selected dinoflagellate transcriptomes and resembled EVEs in terms of proximal gene composition and presence of a characteristic pre-mRNA spliced leader (dinoSL) sequence (as in Levin et al, 2017<sup>57</sup>). Details regarding the collection of samples, generation of metagenomes and associated Symbiodiniaceae amplicon libraries, and associated bioinformatic analyses are provided in Supplementary Fig. 7.

Metagenomic and transcriptomic scaffolds were annotated against a curated database of dinoNAV-like sequences (Supplementary Data 14) via BLASTx (e-value  $< 1 \times 10^{-5}$ ; see Supplementary Fig. 7 for workflow<sup>96</sup>). Alignments to the custom database with a bit score  $< 50$  and percent shared amino acid identity  $< 30\%$  were excluded from further analysis. A length penalty was not imposed during this step due to the limited length of assembled scaffolds (average N50 =  $3341 \pm 127$  nt across all queried libraries). Open reading frames (ORFs) from selected scaffolds were called via Prodigal (v.2.6.3<sup>97</sup>) and annotated against the NCBI-nr database (e-value  $< 0.001$ ; DIAMOND v.2.0.6<sup>98</sup>) to confirm homology to dinoNAVs and to identify adjacent dinoflagellate sequences (e-value  $< 1 \times 10^{-5}$ , bit $\geq 50$ ). In the absence of complete ORFs (potentially due to the limited size of scaffolds, partial integrations, etc.), homology was confirmed through comparison of the initial alignments to the curated database and 300nt of upstream/downstream flanking sequences (bedtools v.2.30.0<sup>99</sup>) against the NCBI-nr database (e-value  $< 0.001$ ; DIAMOND v.2.0.6<sup>98</sup>). This served as further curation and verification, as EVEs can exist in fragmented or degraded states. Non-normalized quality-controlled reads were mapped via bbmap (v.38.84<sup>100</sup>), and putative EVEs were assessed for uniform read coverage across scaffolds, reducing the probability of chimeric assembly. RNA secondary structure was predicted via mfold (v.3.5<sup>101</sup>).

#### dinoNAV EVEs in dinoflagellate and aposymbiotic cnidarian genomes.

Publicly available dinoflagellate and aposymbiotic (dinoflagellate-free) cnidarian genome assemblies were queried to resolve the putative host(s) of dinoNAVs, to assess homology among detected dinoNAVs within coral holobionts, and to compare genes proximal to dinoNAV EVEs in different host species/strains. A chromosome-scale dinoflagellate genome assembly generated from a *Symbiodinium microadriaticum* culture (Accession: GSE152150)<sup>82</sup>, and scaffold-scale genome assemblies were examined for dinoNAV EVEs (Supplementary Data 1B, Supplementary Fig. 7). Scaffold-scale genome assemblies were from the closely related families Symbiodiniaceae and Suessiaceae, and included representatives from the genera *Symbiodinium* ( $n = 9$ ), *Breviolum* ( $n = 1$ ), *Cladocopium* ( $n = 3$ ), *Durusdinum* ( $n = 1$ ), *Fugacium* ( $n = 2$ ), and *Polarella* ( $n = 2$ ), as well as 25 aposymbiotic cnidarian genome assemblies, including the stony coral genera *Acropora* ( $n = 13$ ), *Astreopora* ( $n = 1$ ), *Galaxea* ( $n = 1$ ), *Montastraea* ( $n = 1$ ), *Montipora* ( $n = 3$ ), *Orbicella* ( $n = 1$ ), *Pocillopora* ( $n = 2$ ), *Porites* ( $n = 1$ ), and *Stylophora* ( $n = 1$ ), and the jellyfish *Clytia* ( $n = 1$ ; Fig. 2, Supplementary Data 1B). All publicly available genome assemblies had undergone a form of microbial decontamination, trimming, and quality control prior to assembly, minimizing risk of microbial contamination. Genome completeness and quality further were assessed via BUSCO (v3)<sup>102</sup> with the Eukaryota dataset and QUAST (v5.0.2<sup>103</sup>), respectively. Scaffolds/chromosomes containing putative dinoNAV EVEs were

identified by aligning sequences to the protein version of the Reference Viral DataBase (RVDB v.19<sup>104</sup>) using DIAMOND BLASTx (v0.9.30)<sup>98</sup>. The same exclusion criteria were maintained for alignments of metagenomic scaffolds, also omitting alignments  $< 100$  amino acids. Regions of dinoflagellate genomes exhibiting similarity to the MCP or RdRp of reef-associated dinoNAV reference genomes<sup>57</sup> or other closely related +ssRNA viruses (Supplementary Data 14) were extracted and re-aligned to the NCBI-nr database to further confirm viral homology.

We tested the relationship between the number of identified dinoNAV EVE-containing scaffolds, dinoflagellate genera, and genome quality metrics using a linear model. Model selection was performed with an F-test (package car, v.3.0.12) and assumptions were visually checked. Pairwise comparisons between genera were conducted using the package emmeans (v.1.7.2). Putative whole dinoNAV-like genomes within scaffolds were identified based on the presence of MCP and RdRp-like sequences on the same scaffold no further than 1.5 Kbp apart (Table 1; Supplementary Fig. 3). IRESPred<sup>105</sup> was utilized to identify internal ribosomal entry sites (IRES) with default parameters on putative dinoNAV EVE with whole sequence integrations.

ORFs were predicted and annotated from dinoNAV EVE-containing scaffolds and all dinoflagellate chromosomes using Prodigal<sup>97</sup> and MAKER2 annotation pipeline<sup>106</sup> with the AUGUSTUS gene prediction software<sup>107</sup>. Translated ORFs were then aligned to hybrid database containing the UniProt/Swiss-Prot database and protein version of RVDB (v.19; DIAMOND-BLASTp). ORFs on putative dinoNAV EVE-containing scaffolds and chromosomes were further annotated using InterProScan (v5.48-83.0, Pfam analysis with default parameters) to identify sequences proximal to putative dinoNAV integrations. The presence of dinoflagellate spliced leaders (“dinoSLs”) were examined within 500nt of dinoNAV EVEs using BLASTn with default parameters (except word size=9, excluding two ambiguous positions as specified in Gonzalez-Pech et al. 2021<sup>83</sup>).

**Phylogenetic analysis of dinoNAV EVEs.** Amino acid-based phylogenetic trees were generated with dinoNAV EVE ORFs (MCP and RdRp) from scaffold-scale genomic assemblies, metagenomes, transcriptomes, and sequences from exogenous and closely related +ssRNA reference viruses (Supplementary Data 1 A, B, Supplementary Data 14). Sequences were aligned using the best fit algorithm determined by MAFFT (v7.464)<sup>108</sup> and reviewed and trimmed manually in MEGA (v7)<sup>109</sup>. Maximum-likelihood trees were generated with IQTREE2<sup>110</sup> using the model determined by ModelFinder<sup>111</sup> and 50,000 parametric bootstraps<sup>112</sup> with nearest neighbor interchange optimization. ORFs from the chromosome-level assembly for *S. microadriaticum* culture CCMP2467 were not included in the phylogeny in order to avoid redundancy with those from the analogous scaffold-level assembly. To calculate dN/dS, ORFs were aligned in Clustal Omega (v.1.2.4), refined in MUSCLE (v.3.6), before using pal2nal (v.14) for codon-based nucleic acid alignment. Evolutionary trajectory was then assessed via CODEML (PAML package, v.4.10.5).

**Statistics and reproducibility.** As indicated throughout the article, metagenomes ( $n = 269$ ) and genomes ( $n = 18$ ) served as technical replicates, and ORFs or full EVE sequences served as comparative ecoevolutionary units (replicates described in Table 1) when available. Negative controls (seawater metagenomes, coral host, etc) were also evaluated. All statistical packages are reported in methods or Supplementary Fig. 7.

**Reporting summary.** Further information on research design and collection permits are available in the Nature Research Reporting Summary linked to this article.

#### Data availability

Metadata are accessible in zenodo: <https://zenodo.org/record/6299409#.Y-ClwuzMKml>. Metagenomes are available via <https://doi.org/10.5281/zenodo.7839794>. Seawater metagenomes are available through the European bioinformatics institute (Tara Oceans; ERP001736) and NCBI (PRJEB1787). NCBI accession numbers for individual holobiont species metagenomes, genome assemblies and reference sequences can be found in Supplementary Data 1B, 3 and 14, respectively.

Received: 20 April 2022; Accepted: 24 April 2023;  
Published online: 01 June 2023

## References

- Johnson, W. E. Endogenous retroviruses in the genomics era. *Annu. Rev. Virol.* **2**, 135–159 (2015).
- Johnson, W. E. Origins and evolutionary consequences of ancient endogenous retroviruses. *Nat. Rev. Microbiol.* **17**, 355–370 (2019).
- Johnson, W. E. Endless forms most viral. *PLoS Genet.* **6**, e1001210 (2010).
- Stoye, J. P. Studies of endogenous retroviruses reveal a continuing evolutionary saga. *Nat. Rev. Microbiol.* **10**, 395–406 (2012).
- Gallot-Lavallée, L. & Blanc, G. A glimpse of nucleo-cytoplasmic large DNA virus biodiversity through the eukaryotic genomics window. *Viruses* **9**, 17 (2017).
- Flynn, P. J. & Moreau, C. S. Assessing the diversity of endogenous viruses throughout ant genomes. *Front Microbiol* **10**, 1139 (2019).
- Horie, M. et al. Endogenous non-retroviral RNA virus elements in mammalian genomes. *Nature* **463**, 84–87 (2010).
- Katzourakis, A. & Gifford, R. J. Endogenous viral elements in animal genomes. *PLoS Genet.* **6**, e1001191 (2010).
- Chiba, S. et al. Widespread endogenization of genome sequences of non-retroviral RNA viruses into plant genomes. *PLoS Pathog.* **7**, e1002146 (2011).
- Chu, H., Jo, Y. & Cho, W. K. Evolution of endogenous non-retroviral genes integrated into plant genomes. *Curr. Plant Biol.* **1**, 55–59 (2014).
- Kojima, S. et al. Virus-like insertions with sequence signatures similar to those of endogenous nonretroviral RNA viruses in the human genome. *Proc Natl Acad Sci.* **118**, <https://doi.org/10.1073/pnas.2010758118> (2021).
- Ballinger, M. J., Bruenn, J. A. & Taylor, D. J. Phylogeny, integration and expression of sigma virus-like genes in *Drosoph.* *Mol. Phylogenetic Evol.* **65**, 251–258 (2012).
- Tomas, N., Zwart, M. P., Forment, J. & Elena, S. F. Shrinkage of genome size in a plant RNA virus upon transfer of an essential viral gene into the host genome. *GBE* **6**, 538–550 (2014).
- Palatini, U. et al. Comparative genomics shows that viral integrations are abundant and express piRNAs in the arboviral vectors *Aedes aegypti* and *Aedes albopictus*. *BMC Genomics* **18**, 512 (2017).
- Wang, L. et al. Endogenous viral elements in algal genomes. *Acta Ocean. Sin.* **33**, 102–107 (2014).
- Jebb, D. et al. Six reference-quality genomes reveal evolution of bat adaptations. *Nature* **583**, 578–584 (2020).
- Moniruzzaman, M., Weinheimer, A. R., Martinez-Gutierrez, C. A. & Aylward, F. O. Widespread endogenization of giant viruses shapes genomes of green algae. *Nature* **588**, 141–145 (2020).
- Skirmuntt, E. C., Escalera-Zamudio, M., Teeling, E. C., Smith, A. & Katzourakis, A. The potential role of Endogenous Viral Elements in the evolution of bats as reservoirs for zoonotic viruses. *Annu. Rev. Virol.* **7**, 103–119 (2020). 092818-015613.
- Roossinck, M. J. The good viruses: viral mutualistic symbioses. *Nat. Rev. Microbiol.* **9**, 99–108 (2011).
- Harrison, E. & Brockhurst, M. A. Ecological and evolutionary benefits of temperate phage: what does or doesn't kill you makes you stronger. *BioEssays* **39**, 1700112 (2017).
- Correa, A. M. S. et al. Revisiting the rules of life for viruses of microorganisms. *Nat. Rev. Microbiol.* **19**, 501–513 (2021).
- Jern, P. & Coffin, J. M. Effects of retroviruses on host genome function. *Annu. Rev. Genet.* **42**, 709–732 (2008).
- Oliveira, N. M., Satija, H., Kouwenhoven, I. A. & Eiden, M. V. Changes in viral protein function that accompany retroviral endogenization. *Proc. Natl Acad. Sci.* **104**, 17506–17511 (2007).
- Feschotte, C. & Gilbert, C. Endogenous viruses: insights into viral evolution and impact on host biology. *Nat. Rev. Genet.* **13**, 283–296 (2012).
- Frank, J. A. & Feschotte, C. Co-option of endogenous viral sequences for host cell function. *COVIRO* **25**, 81–89 (2017).
- Mortelmanns, K., Wang-Johanning, F. & Johanning, G. L. The role of human endogenous retroviruses in brain development and function. *APMIS* **124**, 105–115 (2016).
- Sofuku, K., & Honda, T. Influence of endogenous viral sequences on gene expression. *InTechOpen*. <https://doi.org/10.5772/intechopen.71864> (2018)
- Takahashi, H., Fukuhara, T., Kitazawa, H., & Kormelink, R. Virus latency and the impact on plants. *Front. Microbiol.* **10** <https://doi.org/10.3389/fmicb.2019.02764> (2019).
- Whitfield, Z. J. et al. The diversity, structure, and function of heritable adaptive immunity sequences in the *Aedes aegypti* genome. *Curr. Biol.* **27**, 3511–3519.e7 (2017).
- ter Horst, A. M., Nigg, J. C., Dekker, F. M. & Falk, B. W. Endogenous viral elements are widespread in arthropod genomes and commonly give rise to PIWI-interacting RNAs. *J. Virol.* **93**, e02124–18 (2019).
- Suzuki, Y. et al. Non-retroviral Endogenous Viral Element limits cognate virus replication in *Aedes aegypti* ovaries. *Curr. Biol.* **30**, 3495–3506.e6 (2020).
- Aswad, S. & Katzourakis, A. Paleovirology and virally derived immunity. *Trends Ecol. Evol.* **27**, 627–36 (2012).
- Parker, B. J. & Brisson, J. A. A laterally transferred viral gene modifies aphid wing plasticity. *Curr. Biol.* **29**, 2098–2103.e5 (2019).
- Wilson, W., Francis, I., Ryan, K. & Davy, S. Temperature induction of viruses in symbiotic dinoflagellates. *Aquat. Micro. Ecol.* **25**, 99–102 (2001).
- Aiewsakun, P. & Katzourakis, A. Endogenous viruses: connecting recent and ancient viral evolution. *Virology* **479–480**, 26–37 (2015).
- Belyi, V. A., Levine, A. J. & Skalka, A. M. Sequences from ancestral single-stranded DNA viruses in vertebrate genomes: the parvoviridae and circoviridae are more than 40 to 50 million years old. *J. Virol.* **84**, 12458–62 (2010).
- Gilbert, C. & Feschotte, C. Genomic fossils calibrate the long-term evolution of hepadnaviruses. *PLoS Biol.* **8**, e1000495 (2010).
- Kawasaki, J., Kojima, S., Mukai, Y., Tomonaga, K. & Horie, M. 100-My history of bornavirus infections hidden in vertebrate genomes. *Proc. Natl Acad. Sci.* **118**, e2026235118 (2021).
- Li, Y. Q. et al. Discovery of Flaviviridae-derived endogenous viral elements in shrew genomes provide novel insights into Pestivirus ancient history. *bioRxiv*. 02.11.480044. <https://doi.org/10.1101/2022.02.11.480044> (2022)
- Cui, J. & Holmes, E. C. Endogenous lentiviruses in the ferret genome. *J. Virol.* **86**, 3383–5 (2012).
- Kekesova, Z., Ylinen, L. M., Towers, G. J., Gifford, R. J. & Katzourakis, A. Identification of a RELIK orthologue in the European hare (*Lepus europaeus*) reveals a minimum age of 12 million years for the lagomorph lentiviruses. *Virology* **5**, 7–11 (2009). 384.
- Katzourakis, A., Gifford, R. J., Tristem, M., Gilbert, M. T. & Pybus, O. G. Macroevolution of complex retroviruses. *Science* **18**, 1512 (2009). 325.
- Katzourakis, A. Paleovirology: inferring viral evolution from host genome sequence data. *Philos. Trans. R. Soc.* **368**, 20120493 (2013).
- Patel, M. R., Emerman, M. & Malik, H. S. Paleovirology—ghosts and gifts of viruses past. *COVIRO* **1**, 304–309 (2011).
- Barreat, J. G. N. & Katzourakis, A. Paleovirology of the DNA viruses of eukaryotes. *Trends Microbiol.* **30**, 281–292 (2022).
- Knowlton, N. & Rohwer, F. Multispecies microbial mutualisms on coral reefs: the host as a habitat. *Am. Nat.* **162**, S51–S62 (2003).
- Matthews, J. L. et al. Symbiodiniaceae-bacteria interactions: rethinking metabolite exchange in reef-building corals as multi-partner metabolic networks. *Environ. Microbiol.* **22**, 1675–1687 (2020).
- LaJeunesse, T. C. et al. Systematic revision of symbiodiniaceae highlights the antiquity and diversity of coral endosymbionts. *Curr. Biol.* **28**, 2570–2580.e6. (2018).
- Glynn, P. W. Coral reef bleaching: facts, hypotheses and implications. *Glob. Change Biol.* **2**, 495–509 (1996).
- van Oppen, M. J. H., Leong, J.-A. & Gates, R. D. Coral-virus interactions: a double-edged sword? *Symbiosis* **47**, 1–8 (2009).
- Correa, A. M. S. et al. Viral outbreak in corals associated with an in situ bleaching event: atypical herpes-like viruses and a new Megavirus infecting *Symbiodinium*. *Front Microbiol* **7**, 127 (2016).
- Vega Thurber, R., Payet, J. P., Thurber, A. R. & Correa, A. M. S. Virus-host interactions and their roles in coral reef health and disease. *Nat. Rev. Microbiol.* **15**, 205–216 (2017).
- Messiasz, A. et al. Coral bleaching phenotypes associated with differential abundances of Nucleocytoplasmic Large DNA Viruses. *Front Mar. Sci.* **7**, 555474 (2020).
- Grupstra, C. G. B. et al. Thermal stress triggers productive viral infection of a key coral reef symbiont. *ISME J.* **16**, 1430–1441 (2022).
- Correa, A. M. S., Welsh, R. M. & Vega Thurber, R. L. Unique nucleocytoplasmic dsDNA and +ssRNA viruses are associated with the dinoflagellate endosymbionts of corals. *ISME J.* **7**, 13–27 (2013).
- Weynberg, K. D., Wood-Charlson, E. M., Suttle, C. A. & van Oppen, M. J. H. Generating viral metagenomes from the coral holobiont. *Front Microbiol* **5**, 206 (2014).
- Levin, R. A., Voolstra, C. R., Weynberg, K. D. & van Oppen, M. J. H. Evidence for a role of viruses in the thermal sensitivity of coral photosymbionts. *ISME J.* **11**, 808–812 (2017).
- Montalvo-Proaño, J., Buerger, P., Weynberg, K. D. & van Oppen, M. J. H. A PCR-Based Assay targeting the major capsid protein gene of a Dinorna-Like ssRNA virus that infects coral photosymbionts. *Front. Microbiol* **8**, 1665 (2017).
- Nagasaki, K. et al. Comparison of genome sequences of single-stranded RNA viruses infecting the bivalve-killing dinoflagellate *Heterocapsa circularisquama*. *Appl. Environ. Microbiol.* **71**, 8888–8894 (2005).

60. Lawrence, S. A., Davy, J. E., Aeby, G. S., Wilson, W. H. & Davy, S. K. Quantification of virus-like particles suggests viral infection in corals affected by *Porites* tissue loss. *Coral Reefs* **33**, 687–691 (2014).

61. Zhang, H., Zhuang, Y., Gill, J. & Lin, S. Proof that dinoflagellate Spliced Leader (DinoSL) is a useful hook for fishing dinoflagellate transcripts from mixed microbial samples: *Symbiodinium kawagutii* as a case study. *Protist* **164**, 510–527 (2013).

62. Voolstra, C. R. et al. Comparative analysis of the genomes of *Stylophora pistillata* and *Acropora digitifera* provides evidence for extensive differences between species of corals. *Sci. Rep.* **7**, 17583 (2017).

63. Buitrago-López, C., Mariappan, K. G., Cárdenas, A., Gegner, H. M. & Voolstra, C. R. The Genome of the Cauliflower Coral *Pocillopora verrucosa*. *Genome Biol. Evol.* **12**, 1911–1917 (2020).

64. Cunning, R., Bay, R. A., Gillette, P., Baker, A. C. & Taylor-Knowles, N. Comparative analysis of the *Pocillopora damicornis* genome highlights role of immune system in coral evolution. *Sci. Rep.* **8**, 16134 (2018).

65. Helmkampf, M., Bellinger, M. R., Geib, S. M., Sim, S. B. & Takabayashi, M. Draft Genome of the Rice Coral *Montipora capitata* Obtained from Linked-Read Sequencing. *Genome Biol. Evol.* **11**, 2045–2054 (2019).

66. Kitchen, S. A. et al. Genomic variants among threatened acropora corals. *G3 (Bethesda)* **9**, 1633–1646 (2019).

67. ReFuGe 2020 Consortium. The ReFuGe 2020 Consortium—using “omics” approaches to explore the adaptability and resilience of coral holobionts to environmental change. *Front. Mar. Sci.* **2**. <https://doi.org/10.3389/fmars.2015.00068> (2015).

68. Shinzato, C. et al. Eighteen coral genomes reveal the evolutionary origin of acropora strategies to accommodate environmental changes. *Mol. Biol. Evol.* **4**, 16–30 (2021). 38.

69. Ying, H. et al. Comparative genomics reveals the distinct evolutionary trajectories of the robust and complex coral lineages. *Genome Biol.* **2**, 175 (2018). 19.

70. Tara Oceans Consortium Coordinators. et al. Open science resources for the discovery and analysis of Tara Oceans data. *Sci. Data* **2**, 150023 (2015).

71. Littman, R. A., van Oppen, M. J. H. & Willis, B. L. Methods for sampling free-living *Symbiodinium* (zooxanthellae) and their distribution and abundance at Lizard Island (Great Barrier Reef). *J. Exp. Mar. Biol. Ecol.* **364**, 48–53 (2008).

72. Scheufens, T., Iglesias-Prieto, R. & Enriquez, S. Changes in the number of symbionts and *Symbiodinium* cell pigmentation modulate differentially coral light absorption and photosynthetic performance. *Front. Mar. Sci.* **4**, 309 (2017).

73. Fujise, L. et al. Unlocking the phylogenetic diversity, primary habitats, and abundances of free-living Symbiodiniaceae on a coral reef. *Mol. Ecol.* **30**, 343–360 (2021).

74. Grupstra, C. G. B., Rabbitt, K. M., Howe-Kerr, L. I. & Correa, A. M. S. Fish predation on corals promotes the dispersal of coral symbionts. *Anim. Microbiome* **3**, 25 (2021).

75. Sunagawa, S. et al. Ocean plankton. Structure and function of the global ocean microbiome. *Science* **348**, 1261359 (2015).

76. Muller, E. M., Bartels, E. & Baums, I. B. Bleaching causes loss of disease resistance within the threatened coral species *Acropora cervicornis*. *eLife* **7**, e35066 (2018).

77. Janouškovec, J. et al. Major transitions in dinoflagellate evolution unveiled by phylogenomic transcriptomics. *Proc. Natl Acad. Sci.* **114**, E171–E180 (2017).

78. Stephens, T. G. et al. Genomes of the dinoflagellate *Poarella glacialis* encode tandemly repeated single-exon genes with adaptive functions. *BMC Biol.* **18**, 56 (2020).

79. Tan, Y. T. R. et al. Endosymbiont diversity and community structure in *Porites lutea* from Southeast Asia are driven by a suite of environmental variables. *Symbiosis* **80**, 269–277 (2020).

80. Qin, Z. et al. Diversity of Symbiodiniaceae in 15 coral species from the Southern South China Sea: potential relationship with coral thermal adaptability. *Front Microbiol* **10**, 2343 (2019).

81. Sievers, F. et al. Fast, scalable generation of high-quality protein multiple sequence alignments using Clustal Omega. *Mol. Syst. Biol.* **7**, 539 (2011).

82. Nand, A. et al. Genetic and spatial organization of the unusual chromosomes of the dinoflagellate *Symbiodinium microadriaticum*. *Nat. Genet.* **53**, 618–629 (2021).

83. González-Pech, R. A. et al. Comparison of 15 dinoflagellate genomes reveals extensive sequence and structural divergence in family Symbiodiniaceae and genus *Symbiodinium*. *BMC Biol.* **19**, 73 (2021).

84. Zhang, H., Hou, Y., Miranda, L. & Lin, S. Spliced leader RNA trans-splicing in dinoflagellates. *Proc. Natl Acad. Sci.* **104**, 4618–4623 (2007).

85. Lidie, K. B. & van Dolah, F. M. Spliced leader RNA-mediated trans-splicing in a dinoflagellate, *Karenia brevis*. *J. Eukaryot. Microbiol.* **54**, 427–35 (2007).

86. Song, B., Chen, S. & Chen, W. Dinoflagellates, a unique lineage for retrogene research. *Front. Microbiol.* **9**, 1556 (2018).

87. Elbarbary, R. A., Lucas, B. A., Maquat, L. E. Retrotransposons as regulators of gene expression. *Science* **12**, 351(6274):aac7247 (2016)

88. Mita, P. & Boeke, J. D. How retrotransposons shape genome regulation. *Curr. Opin. Genet. Dev.* **37**, 90–100 (2016).

89. Liu, H. et al. *Symbiodinium* genomes reveal adaptive evolution of functions related to coral-dinoflagellate symbiosis. *Commun. Biol.* **1**, 95 (2018).

90. Holmes, E. C. The evolution of endogenous viral elements. *Cell Host Microbe* **10**, 368–377 (2011).

91. Baumgarten, S. et al. Integrating microRNA and mRNA expression profiling in *Symbiodinium microadriaticum*, a dinoflagellate symbiont of reef-building corals. *BMC Genomics* **14**, 704 (2013).

92. Lipardi, C. & Paterson, B. M. Identification of an RNA-dependent RNA polymerase in *Drosophila* involved in RNAi and transposon suppression. *Proc. Natl Acad. Sci.* **106**, 15645–15650 (2009).

93. Blair, C. D., Olson, K. E., & Bonizzoni, M. The Widespread occurrence and potential biological roles of endogenous viral elements in insect genomes. *Curr. Issues Mol. Biol.* **34**, 13–30 (2020).

94. Yan, N. & Chen, Z. Intrinsic antiviral immunity. *Nat. Immunol.* **13**, 214–222 (2012).

95. Pesant, S. et al. (2020). Tara Pacific samples provenance and environmental context—version 2. Zenodo. <https://doi.org/10.5281/zenodo.4068293> (2020).

96. Altschul, S. F., Gish, W., Miller, W., Myers, E. W. & Lipman, D. J. Basic local alignment search tool. *J. Mol. Biol.* **215**, 403–410 (1990).

97. Hyatt, D. et al. Prodigal: prokaryotic gene recognition and translation initiation site identification. *BMC Bioinform.* **11**, 119 (2010).

98. Buchfink, B., Xie, C. & Huson, D. H. Fast and sensitive protein alignment using DIAMOND. *Nat. Methods* **12**, 59–60 (2015).

99. Quinlan, A. R. & Hall, I. M. BEDTools: a flexible suite of utilities for comparing genomic features. *Bioinformatics* **26**, 841–842 (2010).

100. Bushnell, B., Rood, J. & Singer, E. BBMerge—accurate paired shotgun read merging via overlap. *PLOS ONE* **12**, e0185056 (2017).

101. Zuker, M. Mfold web server for nucleic acid folding and hybridization prediction. *Nucleic Acids Res.* **31**, 3406–3415 (2003).

102. Simão, F. A., Waterhouse, R. M., Ioannidis, P., Kriventseva, E. V. & Zdobnov, E. M. BUSCO: assessing genome assembly and annotation completeness with single-copy orthologs. *Bioinformatics* **31**, 3210–3212 (2015).

103. Gurevich, A., Saveliev, V., Vyahhi, N. & Tesler, G. QUAST: quality assessment tool for genome assemblies. *Bioinformatics* **29**, 1072–1075 (2013).

104. Bigot, T., Temmam, S., Pérot, P. & Eloït, M. RVDB-prot, a reference viral protein database and its HMM profiles. *F1000 Res.* **8**, 530 (2020).

105. Kolekar, P. et al. IRESPred: web server for prediction of cellular and viral internal ribosome entry site. *IRES. Sci. Rep.* **6**, 27436 (2016).

106. Holt, C. & Yandell, M. MAKER2: an annotation pipeline and genome-database management tool for second-generation genome projects. *BMC Bioinform.* **12**, 491 (2011).

107. Stanke, M. et al. AUGUSTUS: ab initio prediction of alternative transcripts. *Nucleic Acids Res.* **34**, W435–W439 (2006). (Web Server).

108. Katoh, K. & Standley, D. M. MAFFT multiple sequence alignment software version 7: improvements in performance and usability. *Mol. Biol. Evol.* **30**, 772–780 (2013).

109. Kumar, S., Stecher, G. & Tamura, K. MEGA7: molecular evolutionary genetics analysis version 7.0 for bigger datasets. *Mol. Biol. Evol.* **33**, 1870–1874 (2016).

110. Minh, B. Q. et al. IQ-TREE 2: new models and efficient methods for phylogenetic inference in the genomic era. *Mol. Biol. Evol.* **37**, 1530–1534 (2020).

111. Kalyaanamoorthy, S., Minh, B. Q., Wong, T. K. F., von Haeseler, A. & Jermiin, L. S. ModelFinder: fast model selection for accurate phylogenetic estimates. *Nat. Methods* **14**, 587–589 (2017).

112. Hoang, D. T., Chernomor, O., von Haeseler, A., Minh, B. Q. & Vinh, L. S. UFBoot2: improving the ultrafast bootstrap approximation. *Mol. Biol. Evol.* **35**, 518–522 (2018).

113. Aranda, M. et al. Genomes of coral dinoflagellate symbionts highlight evolutionary adaptations conducive to a symbiotic lifestyle. *Sci. Rep.* **6**, 39734 (2016).

114. Shoguchi, E. et al. Two divergent *Symbiodinium* genomes reveal conservation of a gene cluster for sunscreen biosynthesis and recently lost genes. *BMC Genomics* **19**, 458 (2018).

115. Shoguchi, E. et al. Draft assembly of the *Symbiodinium minutum* nuclear genome reveals dinoflagellate gene structure. *Curr. Biol.* **23**, 1399–1408 (2013).

116. Robbins, S. J. et al. A genomic view of the reef-building coral *Porites lutea* and its microbial symbionts. *Nat. Microbiol.* **4**, 2090–2100 (2019).

117. Shoguchi, E. et al. A new dinoflagellate genome illuminates a conserved gene cluster involved in sunscreen biosynthesis. *GBE* **13**, evaa235 (2021).

118. Lin, S. et al. The *Symbiodinium kawagutii* genome illuminates dinoflagellate gene expression and coral symbiosis. *Science* **350**, 691–694 (2015).

119. Hume, B. C. C. et al. SymPortal: A novel analytical framework and platform for coral algal symbiont next-generation sequencing ITS2 profiling. *Mol. Ecol. Resour.* **19**, 1063–1080 (2019).

## Acknowledgements

Special thanks to the Tara Ocean Foundation, the R/V Tara crew and the Tara Pacific Expedition Participants (<https://doi.org/10.5281/zenodo.3777760>). Thank you also to Carsten G.B. Grupstra and Clark Hamor for their input regarding analyses. We are keen to thank the commitment of the following institutions for their financial and scientific support that made this unique Tara Pacific Expedition possible: CNRS, PSL, CSM, EPHE, Genoscope, CEA, Inserm, Université Côte d'Azur, ANR, agnès b., UNESCO-IOC, the Veolia Foundation, the Prince Albert II de Monaco Foundation, Région Bretagne, Billerudkorsnas, AmerisourceBergen Company, Lorient Agglomération, Oceans by Disney, L'Oréal, Biotherm, France Collectivités, Fonds Français pour l'Environnement Mondial (FFEM), Etienne Bourgois, FRANCE GENOMIQUE (#ANR-10-INBS-09 to P.W.), and the Tara Ocean Foundation teams. Tara Pacific would not exist without the continuous support of the participating institutes. This research is further supported by NSF OCE #2145472 to AMSC, NSF DOB Grant 2025457 to RLVT, and with additional support from NSF PRFB #1907184 to KSIB.

## Author contributions

A.J.V. and K.S.I.B. contributed equally to this study. K.S.I.B. identified endogenization in metagenomes with support from RVT; A.J.V. confirmed the presence in genomes, with support from AMSC. All other authors (C.R.V., B.C.C.H., H.J.R., S.P., D.A., E.B., C.M., G.B., P.W., J.P., G.I., S.R., S.A., B.B., E.B., C.B., C.d.V., E.D., M.F., D.F., P.F., P.G., E.G., F.L., S.P., S.R., S.S., O.T., R.T., D.Z.) are contributing members of the Tara Pacific Expedition, collecting biosamples for metagenomics used in this study or guiding the expedition, with essential bioinformatic support in metagenomic assembly from HJR/SS, sequencing support from PW and JP, and ITS2 analysis from CRV/BCC. A.V., K.S.I.B., A.M.S.C., and R.V.T. wrote the manuscript. This is publication number #26 of the Tara Pacific Consortium.

## Competing interests

The authors declare no competing interests.

## Additional information

**Supplementary information** The online version contains supplementary material available at <https://doi.org/10.1038/s42003-023-04917-9>.

**Correspondence** and requests for materials should be addressed to Kalia S. I. Bistolas.

**Peer review information** *Communications Biology* thanks Guan-Zhu Han, Raúl González-Pech and the other, anonymous, reviewer(s) for their contribution to the peer review of this work. Primary Handling Editor: Zhijuan Qiu and Gene Chong.

**Reprints and permission information** is available at <http://www.nature.com/reprints>

**Publisher's note** Springer Nature remains neutral with regard to jurisdictional claims in published maps and institutional affiliations.



**Open Access** This article is licensed under a Creative Commons Attribution 4.0 International License, which permits use, sharing, adaptation, distribution and reproduction in any medium or format, as long as you give appropriate credit to the original author(s) and the source, provide a link to the Creative Commons license, and indicate if changes were made. The images or other third party material in this article are included in the article's Creative Commons license, unless indicated otherwise in a credit line to the material. If material is not included in the article's Creative Commons license and your intended use is not permitted by statutory regulation or exceeds the permitted use, you will need to obtain permission directly from the copyright holder. To view a copy of this license, visit <http://creativecommons.org/licenses/by/4.0/>.

© The Author(s) 2023

<sup>1</sup>BioSciences Department, Rice University, Houston, TX, USA. <sup>2</sup>Microbiology Department, Oregon State University, Corvallis, OR, USA.

<sup>3</sup>Department of Biology, University of Konstanz, Konstanz, Germany. <sup>4</sup>Department of Biology, Institute of Microbiology and Swiss Institute of Bioinformatics, Vladimir-Prelog-Weg 4, ETH Zürich, CH-8093 Zürich, Switzerland. <sup>5</sup>PSL Research University: EPHE-UPVD-CNRS, USR 3278 CRIobe, Laboratoire d'Excellence CORAIL, Université de Perpignan, 52 Avenue Paul Alduy, 66860 Perpignan, Cedex, France. <sup>6</sup>Centre Scientifique de Monaco, 8 Quai Antoine Ier, Monaco MC-98000, Principality of Monaco. <sup>7</sup>Génomique Métabolique, Genoscope, Institut François Jacob, CEA, CNRS, Univ Evry, Université Paris-Saclay, Evry, France. <sup>8</sup>Research Federation for the study of Global Ocean Systems Ecology and Evolution, FR2022/ Tara Oceans-GOSEE, 3 rue Michel-Ange, 75016, Paris, France. <sup>9</sup>Fondation Tara Océan, Base Tara, 8 rue de Prague, 75012 Paris, France.

<sup>10</sup>School of Marine Sciences, University of Maine, Orono, ME, USA. <sup>11</sup>Sorbonne Université, CNRS, Station Biologique de Roscoff, AD2M, UMR 7144 ECOMAP, Roscoff, France. <sup>12</sup>Shimoda Marine Research Center, University of Tsukuba, 5-10-1 Shimoda, Shizuoka, Japan. <sup>13</sup>Institut de Biologie de l'Ecole Normale Supérieure (IBENS), Ecole normale supérieure, CNRS, INSERM, Université PSL, 75005 Paris, France. <sup>14</sup>Laboratoire des Sciences du Climat et de l'Environnement, LSCE/IPSL, CEA-CNRS-UVSQ, Université Paris-Saclay, F-91191 Gif-sur-Yvette, France. <sup>15</sup>Weizmann Institute of Science, Department of Earth and Planetary Sciences, 76100 Rehovot, Israel. <sup>16</sup>Université Côte d'Azur, CNRS, INSERM, IRCAN, Medical School, Nice, France. <sup>17</sup>Laboratoire International Associé Université Côte d'Azur-Centre Scientifique de Monaco, LIA ROPSE, Monaco, France. <sup>18</sup>Sorbonne Université, CNRS, Laboratoire d'Ecogéochimie des Environnements Benthiques (LECOB), Observatoire Océanologique de Banyuls, 66650 Banyuls sur mer, France. <sup>19</sup>Department of Medical Genetics, CHU of Nice, Nice, France. <sup>20</sup>Sorbonne Université, Institut de la Mer de Villefranche sur mer, Laboratoire d'Océanographie de Villefranche, F-06230 Villefranche-sur-Mer, France.

<sup>21</sup>European Molecular Biology Laboratory, European Bioinformatics Institute, Wellcome Genome Campus, Hinxton, Cambridge CB10 1SD, UK.

<sup>22</sup>School of Biological and Chemical Sciences, Ryan Institute, University of Galway, University Road H91 TK33, Galway, Ireland. <sup>23</sup>These authors contributed equally: Alex J. Veglia, Kalia S.I. Bistolas. ✉email: [ksb97@cornell.edu](mailto:ksb97@cornell.edu)